

Simulation and experimental study on drag reduction and anti-adhesion of subsoiler with bionic surface

Jiping Niu¹, Tongyun Luo², Jiaqing Xie^{2*}, Haoxuan Cai², Zhikang Zhou², Jun Chen², Shuo Zhang²

(1. College of Water Resources and Architectural Engineering, Northwest A&F University, Yangling 712100, Shaanxi, China;

2. College of Mechanical and Electronic Engineering, Northwest A&F University, Yangling 712100, Shaanxi, China)

Abstract: A new subsoiler with placoid scale microstructure bionic surface was proposed which mimicked shark skin to reduce tillage resistance and soil adhesion during subsoiling cultivation. The contour curves of placoid scale microstructure on shark skin were fitted, and two kinds of bionic subsoiler with continuous and discontinuous microstructures were designed and fabricated, respectively. The effects of different bionic surfaces on tillage resistance were investigated by finite element simulation and experiment. The results indicated that the bionic subsoiler with discontinuous microstructure reduced the horizontal and vertical force by 21.3% and 24.8%, respectively. The subsoiler with discontinuous microstructure surface can prevent the adhesion between the soil and subsoiler surface more efficiently.

Keywords: drag reduction, anti-adhesion, subsoiler, bionic surface, placoid scale microstructure, finite element simulation

DOI: 10.25165/j.ijabe.20221504.6531

Citation: Niu J P, Luo T Y, Xie J Q, Cai H X, Zhou Z K, Chen J, et al. Simulation and experimental study on drag reduction and anti-adhesion of subsoiler with bionic surface. *Int J Agric & Biol Eng*, 2022; 15(4): 57–64.

1 Introduction

Subsoiling cultivation is an effective method to promote crop growth and enhance the sustainable development capacity of agriculture^[1-4]. The subsoiler is divided into three types of the two-wing subsoiler, arrow subsoiler and chisel subsoiler according to their structures^[5,6]. At present, the main problems of subsoiling cultivation come from the large cultivation resistance and serious energy consumption. The tillage depth of subsoiler could reach 45 cm, so the tillage machine with high horsepower is essential. Due to the large traction force subjected on the subsoiler surface, as well as the strong adhesion of soil particles, which affected the load stability and further increased the wear of subsoiler. Therefore, it is necessary to develop a new subsoiler to reduce tillage resistance and inhibit adhesion. The drag reduction methods include electron osmosis drag reduction, vibration drag reduction, magnetization drag reduction, bionic drag reduction and structure optimization of the subsoiler components.

Bionic surface tillage reduction was one of the most promising drag reduction methods. Recently, biomimetic technology had been widely applied in agricultural equipment due to the ability to

reduce tillage resistance and prevent adhesion^[7-9]. Huang et al.^[10] developed a kind of bionic viscosity reduction of chisel type energy saving subsoiling shovel based on scale structure of pangolin, which solves the problems of clay and high resistance in traditional subsoiling process. The results showed that the number of bionic surfaces, forward speed and coating materials had no significant effect on the traction resistance; the number of bionic surfaces and coating materials had a significant effect on soil adhesion; the forward speed had a significant impact on soil adhesion. Zhang et al.^[11,12] designed a bionic anti-drag subsoiler based on the structure of *Mus musculus*' claw toe, the anti-drag subsoiler had exponential curve shape of soil-cutting edge of shaft. The tillage resistances of bionic anti-drag subsoiler were reduced by 8.5% to 39.5%, respectively. Jia et al.^[13] designed a hare claw toe bionic shallow-loosening shovel and a pangolin scale bionic ridging shovel with anti-drag functions, the field verification tests confirmed that these two bionic tillage devices outperformed the conventional tillage device in reducing tractive drag by 13%-19%. Zhao et al.^[14] designed a bionic stubble-deep loosening combined tillage machine through bionic prototype analysis, coupled bionic analysis, coupled bionic design, theoretical analysis and application of intelligent control techniques. Based on the unique biology of the hare's paws, toes and nails, the bionic self-excited vibration deep loosening device adopted a new series-parallel composite bionic elastic system and an intelligent tilling depth control system with a fuzzy algorithm, which significantly improved the tilling depth consistency ($p < 0.05$). In addition, the geometric structure of *Chlamys farreri* surface was used to improve the wear resistance of subsoiling blade, it is found that the outer surface of the *Chlamys farreri* flap has a radial rib structure, which has a guiding and rolling effect on the abrasive particles sliding on its surface and reduces the ploughing of the abrasive particles on the worn surface, thus reducing the abrasive damage to the surface. Tong et al.^[15] applied the texture of shell surface to agricultural machinery which interacted with soil to improve the wear resistance of soil touching parts, the effects of biomimetic designs of tine furrow opener surface on equivalent pressure and pressure in the direction of

Received date: 2021-02-18 **Accepted date:** 2022-02-07

Biographies: **Jiping Niu**, PhD, Lecturer, research interests: agricultural soil and water environment, Email: niujp@nwafu.edu.cn; **Tongyun Luo**, MS candidate, research interests: intelligent agricultural equipment technology, Email: luckycamel@foxmail.com; **Haoxuan Cai**, MS candidate, research interests: potato sowing technology and equipment, Email: caihaoxuan1998@nwafu.edu.cn; **Zhikang Zhou**, MS candidate, research interests: advanced manufacturing of functional surfaces, Email: zhouzk@bit.edu.cn; **Jun Chen**, PhD, Professor, research interests: intelligent agricultural equipment technology and vehicle performance testing, Email: chenjun_jdxy@nwafu.edu.cn; **Shuo Zhang**, PhD, Associate Professor, research interests: intelligent agricultural machinery equipment and intelligent vehicle control, Email: zhangshuo@nwafu.edu.cn.

***Corresponding author:** **Jiaqing Xie**, PhD, Lecturer, research interests: advanced manufacturing technology. College of Mechanical and Electronic Engineering, Northwest A&F University, Yangling 712100, Shaanxi, China. Tel: +86-29-87091867, Email: xiejq@nwafu.edu.cn.

motion on opener surface against soil were studied, the experimental results showed that furrow opener with biomimetic tubular section ridges recorded the lowest pressure. The surface of shark skin was scaly and had a non-smooth pelagic structure similar to round valley, the direction of pelagic groove was parallel to the swimming direction^[16]. The groove structure on the surface of shark skin effectively reduced the resistance of shark body when swimming^[17], as it optimized the fluid structure of the fluid boundary layer on the shark body surface, while simultaneously inhibited and delayed the occurrence of turbulence. At present the shark skin bionics design of drag reduction surface was divided into two types, namely replicate the shield scale structure directly and imitate the shark skin groove. It was possible to apply the surface structure of shark skin to the surface of subsoiler to reduce the cultivation resistance. But now, the related research was very few, the study of shark skin bionics design of subsoiler was much rarer. Pu et al.^[18] investigated the surface morphology, structure and mechanical behaviors of shark skin, and introduced various methods of fabricating biomimetic rib-let-structured surfaces. The drag-reduction mechanism was attributed to the non-smooth surface. Although sharks live in water, the existing studies have proved that the surface microstructure of shark skin has excellent drag reduction characteristics, which can be used in subsoiling drag reduction components. Its convex structure contour is also conducive to shear the soil and prevent adhesion between soil and subsoiler surface. Sun et al.^[19] adopt biomimetic design method to reduce subsoiler energy consumption and soil disturbance. Two kinds of bionic structural elements were inspired by the placoid scale rib structure of shark skin, which had the effect of drag reduction. These elements were then applied to the subsoiler to reduce energy consumption. Then Sun, by means of simulation and analysis, had proved that the subsoiler with bionic structure played a more positive role in reducing resistance and energy consumption than the ordinary subsoiler. However, the microstructure on shark surface was simplified during the modeling process, and the author had not carried out experimental verification.

This research intended to adopt the placoid scale microstructure on shark skin to the subsoiler working surface to reduce tillage resistance and prevent soil adhesion during subsoiling cultivation. The contour curves of placoid scale microstructure on shark skin were fitted, two kinds of bionic subsoiler with continuous and discontinuous structure were designed and fabricated respectively. Then the two different subsoiler effects on reducing tillage resistance were verified by experiments. More precisely, the first is to obtain a piece of skin from the dorsal fin of a hammerhead shark, and the microstructure on the skin was observed by scanning electron microscope (SEM), the contour curves of the microstructure were captured by a laser scanning confocal microscopy (LSCM). Based on the obtained contour curves of the microstructure, two kinds of subsoilers with continuous and discontinuous structure on the surface were designed respectively. And then, the effects of different subsoilers on drag reduction were conducted by Finite element (FE) simulation. Lastly, the designed subsoilers with different bionic structure surfaces were machined by the milling and wire cutting processing. The influences of bionic surfaces on reducing tillage resistance were investigated through experiments.

This study could provide a theoretical basis for enriching the drag reduction and anti-adhesion technology of subsoiling to save energy consumption, as well as promote the development of agricultural technology.

2 Materials and methods

2.1 Observation of shark skin surface

To obtain the distributions of microstructures on shark skin surface and the out-line size of the single microstructure, SEM and LSCM methods were adopted to observe the placoid scale microstructure of a hammerhead shark skin^[20]. The shark skin was dehydrated and fixed before the SEM observation. A piece of skin of 1 cm×1 cm taken from the dorsal fin of a hammerhead shark was washed with an ultrasonic cleaner for 15 min, and then soaked in formalin for fixation. The shark skin used in this experiment was purchased from Laboratory Animal Service Center (Northwest A&F University, China). Gradient dehydration was carried out by anhydrous ethanol with volume fraction of 30%, 50%, 75%, 80%, 95%, 100%^[21], each dehydration step was kept for 15-20 min. Figure 1 shows the observed SEM photograph of microstructures on the dorsal fin of hammerhead shark with the magnifying power of 200 magnifications, the hammerhead shark scale had five keels, and covered evenly. Each shark scale was between 100-300 μm .

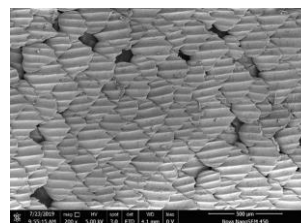


Figure 1 SEM photograph of microstructures on the dorsal fin of hammerhead shark

In order to facilitate the three-dimensional modeling of shark scales, the longitudinal and transverse cross sections of shark scale on hammerhead shark skin were obtained by LSCM. To ensure the accuracy of the microstructure contour curves, the shark skin used in the test was only fixed with formalin. The obtained contour curves are shown in Figure 2, the contour curves of longitudinal and transverse cross sections were irregular. The simplified design of microstructures would not guarantee the drag reduction performance. Therefore, it was necessary to fit the contour curves accurately.

2.2 Soil property test

In order to investigate effect of subsoiler on tillage drag-reduction from two kinds of surface structures, the soil grain-size distribution test and direct shear test were carried out, respectively. The subsoiling experiment was conducted in the laboratory of agricultural machinery, Northwest A&F University^[22,23]. The length, width and height of the soil bin used in this experiment were 20 m, 2.2 m and 1.5 m, respectively. The soil used in the experiment was taken from a corn stubble field in Zhaixi Village in the Yangling Agricultural Demonstration Area, Xianyang, Shaanxi Province, China, on Dec 27, 2019.

The grain-size distributions of the soil were tested by laser diffraction method. The result indicated that the particle size distribution of soil was not affected by the depth, as shown in Table 1. According to the classification standard of soil types, the experimental soil type was clay loamy soil.

Before the subsoiling experiment, the soil in the soil bin was treated by layered treatment to ensure that the soil parameters were consistent with the soil in the field. Firstly, excavate soil in the soil bin with a depth of 20 cm, rotate the remaining soil for three times with a rotary cultivator, then compact it with a vibratory impact rammer. Secondly, spray appropriate amount of water on

the surface of the compacted soil layer, backfill the excavated surface soil evenly (about 10 cm). After 2 d of infiltration, loosen the surface soil completely with a rotary cultivator, and compact it with rollers. Repeat the above steps to backfill the remaining soil (about 10 cm). The average soil moisture content in the soil bin after pretreatment was tested by soil moisture quick tester, and soil hardness was measured by soil hardness tester. The tested average soil moisture content was 18.6%, and the hardness was 5-10 kg/cm² within 20 cm depth, and 10-20 kg/cm² below 20 cm depth. According to the direct shear test, the internal friction angle of soil was 24.1 ° and cohesive force was 30.5 kPa, as shown in Figure 3.

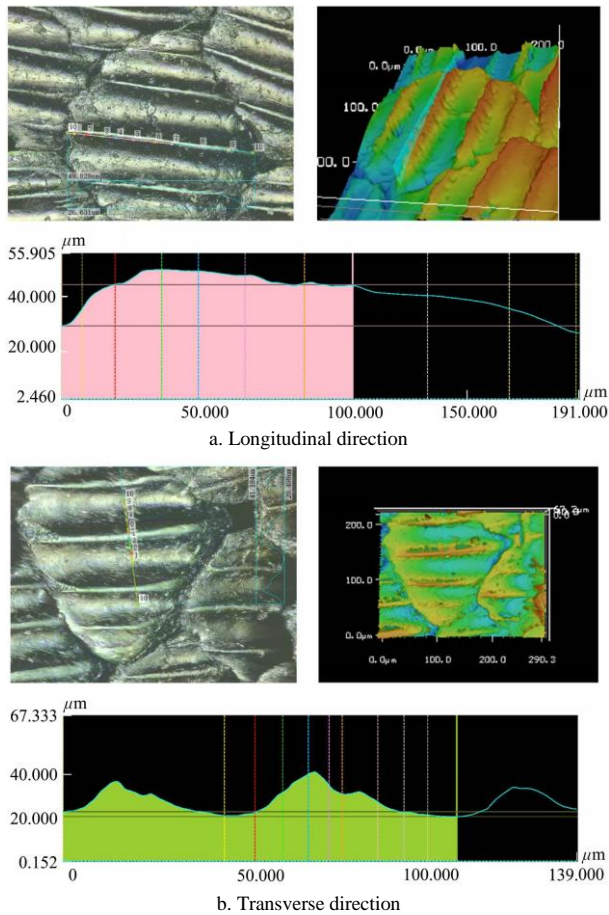


Figure 2 Microstructures of hammerhead shark skin obtained by LSCM on different cross sections

Table 1 Grain-size distributions of the experimental soil

| Soil depth /cm | Clay particle content/% (0.01-2.0 μm) | Silt particle content/% (2.0-20.0 μm) | Sandy particle content/% (20.0-2000.0 μm) |
|----------------|---------------------------------------|---------------------------------------|---|
| 0 | 21.24 | 34.56 | 44.20 |
| 20 | 21.69 | 35.13 | 43.17 |
| 30 | 21.34 | 34.59 | 44.07 |

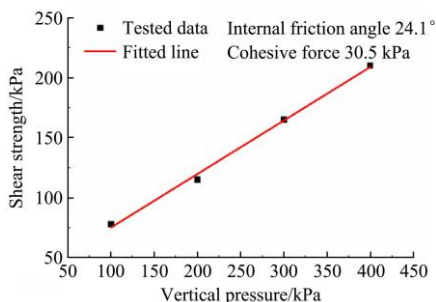


Figure 3 Results of the soil direct shear test

2.3 FE simulation

In order to study the subsoiling cultivation mechanism of different subsoilers, the FE model based on Smoothed Particle Hydrodynamics (SPH) algorithm was established according to the results of soil property tests, the drag reduction effects of the bionic subsoilers were simulated and predicted.

The Mohr-Coulomb criterion was adopted to model the inelastic behavior of soil^[24,25]. The criterion assumed that the yield function was governed by the maximum shear stress (which was dependent on the normal stress) as,

$$\tau_f = c + \sigma \tan \phi \tag{1}$$

where, τ_f is the maximum possible shear stress in an arbitrary plane, kPa; c is the cohesion kPa; σ is the normal effective stress, kPa; ϕ is the angle of internal friction or friction angle, (°).

The measured parameters of soil physical properties are shown in Table 2, and the subsoiler was regarded as rigid in the simulation.

Table 2 The measured parameters of soil physical properties

| Density $\rho/\text{kg m}^{-3}$ | Young's modulus E/MPa | Poisson's ratio λ | Friction angle $\phi/(\text{°})$ | Cohesive force c/kPa |
|---------------------------------|--------------------------------|---------------------------|----------------------------------|-------------------------------|
| 1404 | 50 | 0.3 | 24.1 | 5.2 |

A standard share shaft was used to conduct the subsoiling experiment. The schematic diagram and dimension parameters of subsoiler and share shaft profile after assembly are shown in Figure 4. The subsoiler and share shaft were connected by two bolts. In order to improve the calculation efficiency, the simulation model simplified the two bolts.

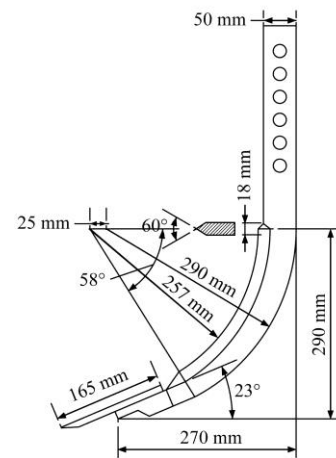


Figure 4 Schematic diagram of subsoiler and share shaft profile after assembly

The SPH algorithm was used to simulate soil deformation during subsoiling process, the element type was C3D8R. The 10 nodes modified rectangular tetrahedron C3D10M were used for the subsoiler. The coarse mesh was used for the share shaft, and the refinement mesh was applied for the subsoiler to ensure the calculation accuracy while promoting the efficiency. The constructed FE simulation model is shown in Figure 5, the tillage depth was 20 cm, an infinite boundary was adopted in the geometric model of soil to eliminate the influence of energy spillover on simulation accuracy. The meshed average grid size was smaller than the minimum size grid of soil part.

2.4 Subsoiling cultivation experiment

To verify the effects of designed bionic subsoilers on drag reduction and anti-adhesion, three kinds of subsoilers were tested. The assembled subsoiler was installed on the soil bin testing vehicle, as shown in Figure 6. The subsoiler was pulled forward

by the soil bin testing vehicle for subsoiling cultivation, and the experimental data during the test process was collected. The sampling frequency was 100 Hz, and the cultivation speed was 2.1 km/h.

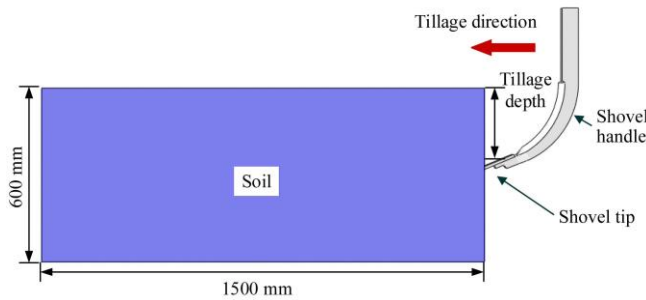


Figure 5 Simulation model of the constructed FE

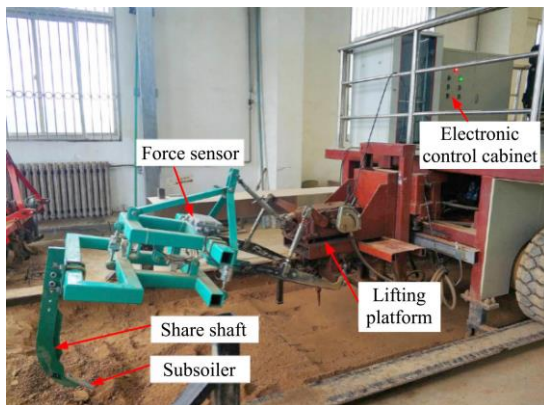


Figure 6 Subsoiling experiment machine

2.5 Characterization

The surface morphology of shark skin was identified by Scanning Electron Microscope (SEM) (BCPCAS4800, Beckman Instruments Inc, America). The microstructure curves on shark skin surface were observed by the laser microscope (VHX-1000, KEYENCE Co., Ltd, Japan) with display resolution of $0.005 \mu\text{m}$ in height and $0.01 \mu\text{m}$ in width. The grain-size distributions of the soil were tested by soil laser particle size analyzer (XCLD-620C, Xiamen Xiuchen Instrument Co., Ltd, China). The soil was pretreated with a rotary cultivator (1GQN-125, China YITUO Group Co., Ltd., China, 12-16 cm deep), and compacted with vibration impact rammer (HCD80, Jining Ouke Industrial and Mining Equipment Co., Ltd., China, impact frequency: 420-650 times/min). The average soil moisture content in the soil bin after pretreatment was tested by soil moisture quick tester (TS-1, Nanjing Soil Instrument Co., Ltd, China), and the soil hardness was measured by soil hardness tester (TE-3, Nanjing Soil Instrument Co., Ltd, China). A high speed milling center (DMU80, Demaji Machine Tool Co., Ltd, Germany) with five axes (maximum spindle speed 24000 r/min) was used to fabricate the subsoilers. The soil bin testing vehicle used in this test was an electric frequency conversion four-wheel drive soil bin testing vehicle (Harbin Bona Technology Co., Ltd, China), including the frame, servo drive motor, force sensor system, electronic control cabinet and lifting platform components^[18]. The 3D modeling software SolidWorks (Dassault Systemes S.A., France) was applied to fabricate the designed bionic subsoiler. The MATLAB (MathWorks, inc., America) software was adopted to fit the longitudinal and transverse profiles of shark scales, and the general FE software ABAQUS (Dassault Systemes S.A., France) was used for the FE simulation.

3 Results and discussion

3.1 Bionic structure construction of shark skin surface

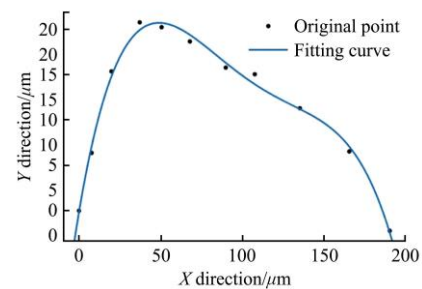
The polynomial fitting method was carried out to fit the longitudinal and transverse profiles of shark scales^[26]. The longitudinal contour y_1 and transverse contour y_2 fitting formulas were expressed as:

$$y_1 = -0.02776x^4 + 11.96x^3 + 1842x^2 + 10730x + 15780 \quad (2)$$

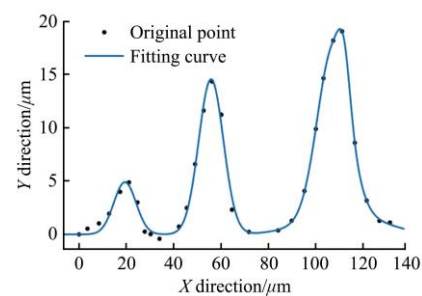
$$y_2 = 4.201e^{-\frac{(x-111.9)^2}{3.519}} + 14.53e^{-\frac{(x-55.74)^2}{7.358}} + 15.52e^{-\frac{(x-107.2)^2}{9.311}} + 1.974e^{-\frac{(x-111.8)^2}{22.07}} + 4.893e^{-\frac{(x-19.39)^2}{6.614}} \quad (3)$$

where, x is the horizontal coordinates.

The longitudinal and transverse contour curves obtained by mathematical fitting are shown in Figure 7. The variance SSE of the two fitted curves were 4.175 and 5.040, R^2 were 0.9934 and 0.9945, respectively. The fitting accuracy of the two curves could meet the accurate requirement of engineering design, the corresponding bionic structure would be designed according to the fitted curve. It is expected that the new subsoiler with placoid scale structure bionic surface can cut and dredge the soil applied on the surface of the subsoiler during subsoiling cultivation, thus reduce the tillage resistance. In addition, there was no pure plane at the grooved style bionic structures, so the soil in contact with the bionic surface is subject to varying normal and shear stress, which reduces the possibility of bonding between the soil and the surface.



a. Longitudinal



b. Transverse

Figure 7 Contour curves obtained by mathematical fitting

In order to analyze the influence of the longitudinal and transverse profiles of shark structures on drag reduction, two kinds of structures were designed, including continuous structure and discontinuous structure, as shown in Figure 8. The fitted transverse contour curve was adopted to fabricate the continuous structure, the longitudinal and transverse contour curves were applied to fabricate the discontinuous structure.

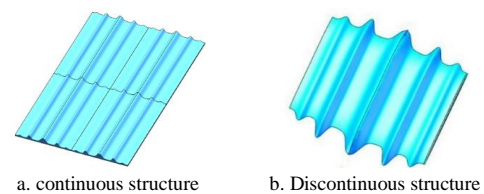
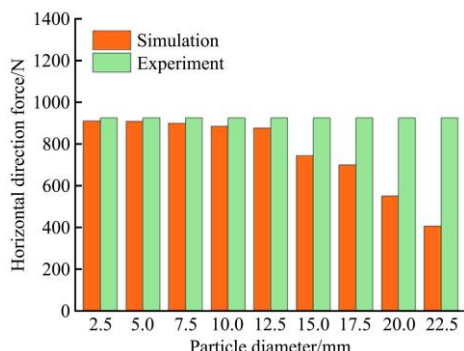


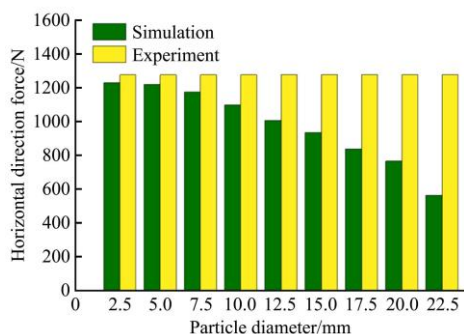
Figure 8 The designed microstructural units

3.2 Subsoiling cultivation simulation based on FE method

SPH method, which based on kernel function approximation, discretized the continuum into a series of particles with mass. SPH method could effectively calculate the large deformation behavior of materials. In order to obtain high simulation accuracy, the influences of partitioned single particle diameter on simulation and experimental results were compared. As shown in Figure 9, the calculation accuracy increased with the decrease of particle diameter. When the particle size was less than 10 mm, to further reduce the particle diameter had limited improvement on calculation accuracy, but greatly increased the computational resources consumption. Based on the above analysis, the soil particle diameter was determined as 10 mm.



a. Horizontal direction



b. Vertical direction

Figure 9 Influences of particle diameter on simulation results

The magnification of bionic microstructure was also a key factor affecting drag reduction capability. The mechanism of drag reduction of shark skin is mainly attributed to the shape and contour of its surface microstructure of placoid scale. In fact, the size of placoid scale microstructure varies with the location and age of hammerhead sharks, and the research on the effect of size on drag reduction is relatively rare. In this study, the new subsoiler with placoid scale structure bionic surface can cut and dredge the soil applied on the surface of the subsoiler during subsoiling cultivation, thus reducing the tillage resistance. In addition, there was no pure plane at the grooved style bionic structures, the soil in contact with the bionic surface is subject to varying normal and shear stress, which reduces the possibility of bonding between the soil and the surface. However, the drag reduction and anti-adhesion performance of the bionic structure surface will be inhibited due to the phenomenon of soil compaction and agglomeration during the subsoiling cultivation. Based on the above analysis, it is well founded that properly enlarging the size of the bionic structure is conducive to reduce the impact of soil compaction and agglomeration on the drag reduction performance of the subsoiler with bionic surface. Therefore, the relationship between the magnification of microstructure and the average tillage resistance through simulation tests was analyzed. The working

process simulation of bionic subsoiler with different magnification was carried out. The effect of microstructure magnification on average resistance force is shown in Figure 10. For the subsoiler with continuous surface, the horizontal and vertical resistance increased with the enlarge of surface microstructure magnification, while for the subsoiler with discontinuous surface, the resistance force at horizontal direction decreased with the magnification, the change tendency of vertical force was not obvious. Based on the above analysis, the unit size of the microstructure was selected to enlarge 75 times. In addition, the enlarged bionic structure is also easier to process, and it is convenient to strengthen the surface to prolong the service life.

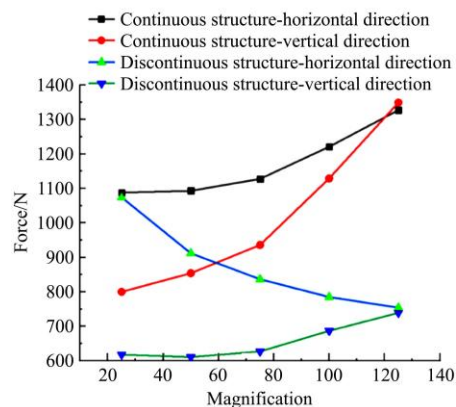
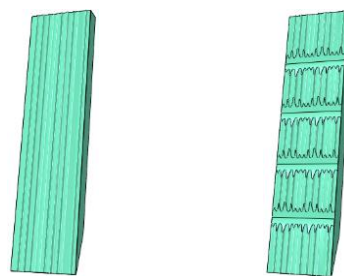


Figure 10 Effects of microstructure magnification on average resistance force

The designed subsoilers with continuous structure and discontinuous structure are shown in Figure 11. In order to facilitate processing and ensure that the soil is easy to flow out of the discontinuous position during subsoiling cultivation, the discontinuous area of each group of bionic structure is kept in a straight line, as shown in Figure 11b.



a. Continuous structure b. Discontinuous structure

Figure 11 The designed subsoiler with different structures

Through the FE simulation, the stress nephogram of traditional subsoiler without bionic structures and newly designed subsoiler with continuous and discontinuous structure surface during subsoiling cultivation were obtained, as shown in Figure 12. Due to the guidance effect of bionic structure, more soil was brought out from the continuous structure of the subsoiler. The soil flow characteristics of subsoiler with discontinuous structure are more complex. The existence of the irregular bionic microstructure on subsoiler surface caused the soil in contact with subsoiler surface bearing the varying forward and tangential pressures at the same time, which made it difficult for the soil to bond to the subsoiler surface. In addition, there was no pure plane at the bottom of the grooved style bionic structures (namely the continuous and discontinuous structure surface), it was also unable to produce adhesion. The soil converging at the bottom was guided by the grooved style bionic structures and moved continuously. Meanwhile, the existence of the grooved style bionic structures was

also conducive to breaking the soil cohesive aggregation as well as improving the soil structure.

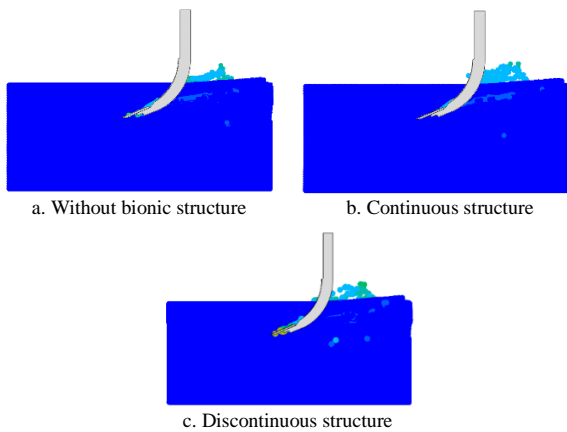
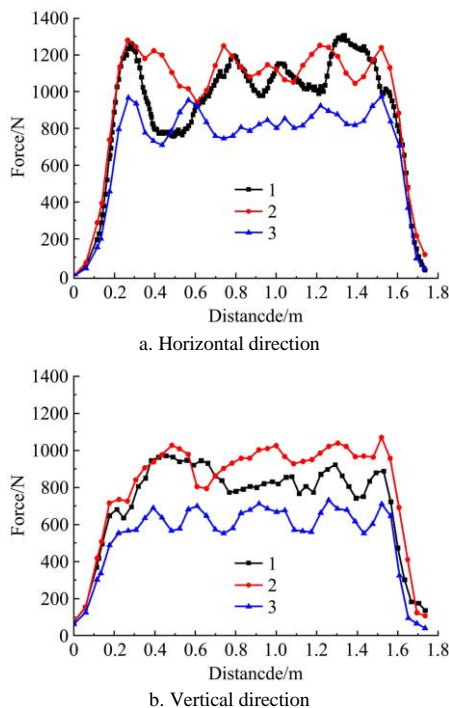


Figure 12 Equivalent stress distribution of three kinds of subsoilers

The horizontal and vertical resistances of the subsoiler were extracted during subsoiling cultivation from the FE simulation, respectively. It was indicated that the designed two kinds of subsoilers with bionic surface both contributed to reducing the horizontal resistance. Figure 13 shows that the mechanical fluctuation of the designed bionic subsoilers was smaller than that of the traditional subsoiler without bionic structures, which was conducive to reducing the load impact and the surface wear, as well as extending the service life. In the vertical direction, the tillage resistance of subsoiler with continuous structure was higher than the traditional subsoiler, but the resistance fluctuation was the smallest in the above-mentioned three kinds of subsoilers. It could be concluded that the subsoiler with continuous microstructure surface had a guiding effect on the soil and reduced the fluctuation of the force, but also increased the vertical resistance, while the vertical resistance of the subsoiler with discontinuous microstructure surface was not significantly increased.



1. Without bionic structure 2. Continuous structure subsoiler
3. Discontinuous structure subsoiler.

Figure 13 Comparison of the tillage resistance obtained in the simulation with three kinds of subsoilers

The simulation results showed that the drag reduction effect of the subsoiler with discontinuous microstructure surface is better than the others. The soil adhesion during subsoil tillage was not considered in the simulation, it was necessary to verify the drag reduction effect of the designed bionic subsoilers by subsoiling cultivation experiment.

3.3 Influence of bionic surface on the subsoiling resistance

In order to verify the drag reduction and anti-adhesion effects of the designed bionic subsoiler, three kinds of subsoilers were prepared and tested. The subsoiler material was X8CRN125-21. The high speed milling method was adopted to fabricate the microstructures on the subsoiler. A bull mill with handle diameter of 6 mm and R1 mm was applied to fabricate the microstructures. The machined three kinds of subsoilers are shown in Figure 14.

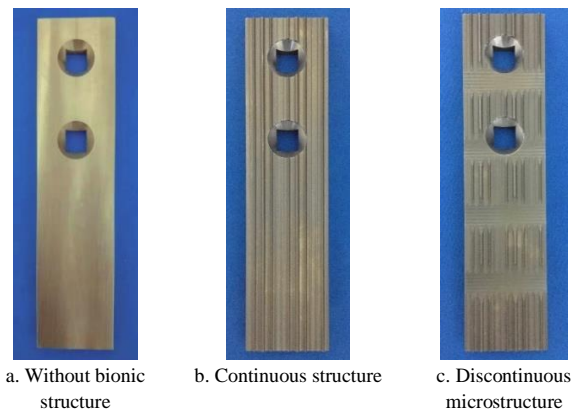
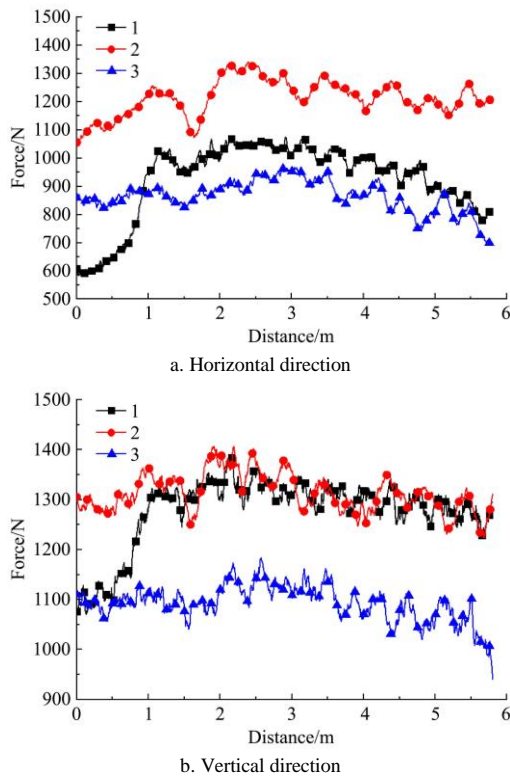


Figure 14 Three kinds of subsoilers machined by CNC process

The comparison of the subsoiler resistance curves obtained in the experiment of three kinds subsoilers is shown in Figure 15. It is found that in the horizontal direction, the resistance of the continuous structure is larger than that of the non-structure subsoiler, and the fluctuation of the force is larger, while the resistance of the discontinuous structure subsoiler is smaller than the non-structure subsoiler. The vertical resistance of the continuous structure subsoiler is basically the same as that of the non-structure subsoiler. The vertical resistance of the subsoiler with discontinuous structure is much smaller than that of the other two subsoilers. The bionic subsoiler with discontinuous microstructure reduced the horizontal and vertical force by 21.3% and 24.8%, respectively. The test results were basically consistent with the simulation results, but the average resistance obtained from the experiment was greater than the simulation results. It is speculated that the soil is bonded to the surface of the subsoiler in the subsoiling cultivation, resulting in the increasing of tillage resistance, which cannot be reflected in the simulation. In addition, the simulation and experimental results show that the three kinds of subsoilers produced stress shaking during the subsoiling cultivation, which is caused by the continuous accumulation and shearing of the soil in contact with the subsoiler surface. The horizontal and vertical direction stresses of the bionic subsoiler with discontinuous structure are significantly reduced, while the frequency of stress shaking is increased and the amplitude is reduced. The discontinuous structure can more easily cut off the soil accumulated on the subsoiler surface and lead out the soil more quickly by the break slot. The pressure fluctuation of subsoiler during subsoiling cultivation is small, which is conducive to improving the smoothness and durability of subsoiling equipment.

After repeating the subsoiling cultivation experiment for ten times, it was found that the soil adhesion existed on the surface of

three kinds of subsoilers, but the subsoiler with discontinuous microstructure surface had the least adhesion. There is no pure plane at the bottom of the grooved style bionic structures. During the subsoiling cultivation, the stress took place on the sites where soil and the bionic structure surface contact with each other was unbalanced, which was difficult to produce adhesion, thus reducing the resistance of subsoiling cultivation. However, the subsoiler with continuous structure hindered the flow of soil to both sides, which increased the resistance of horizontal direction to a certain extent. The effect of soil moisture content on the anti-adhesion effect of subsoiling shovel with different bionic structure surfaces needs to be further studied.



1. Without bionic structure subsoiler 2. Continuous structure subsoiler
3. Discontinuous structure subsoiler.

Figure 15 Comparison of the subsoiler force curves obtained in the experiment of three kinds subsoilers

4 Conclusions

This research adopted the placoid scale microstructure on shark skin to the subsoiler surface to reduce tillage resistance and prevent soil adhesion during subsoiling cultivation. The contour curves of placoid scale microstructure on shark skin were measured and fitted accurately. The bionic subsoilers with continuous and discontinuous structure surfaces were designed respectively, and the effects of bionic subsoilers on drag reduction were investigated by FE simulation and experiment. The research results were summarized as follows:

(1) The bionic surface with discontinuous structure had superiority on drag reduction and reduced stress fluctuation. The cultivation force with continuous structure in the vertical direction was increased compared with that of the traditional subsoiler due to its guidance effect on the soil.

(2) The bionic subsoiler with discontinuous microstructure reduced the horizontal and vertical force by 21.3% and 24.8%, respectively, the bionic surface structure had a positive effect on preventing adhesion between the soil and the subsoiler surface.

Acknowledgements

This work was financially supported by Natural Science Basic Research Program of Shaanxi (Program No. 2021JQ-173), and Innovation and Entrepreneurship Training Program of Northwest A&F University (Program No. 201910712134).

[References]

- [1] França J S, Reichert J M, Holthusen D, Rodrigues M F, De Araújo E F. Subsoiling and mechanical hole-drilling tillage effects on soil physical properties and initial growth of eucalyptus after eucalyptus on steepplands. *Soil and Tillage Research*, 2020; 207: 104860. doi: 10.1016/j.still.2020.104860.
- [2] Ahmadi I. A power estimator for an integrated active-passive tillage machine using the laws of classical mechanics. *Soil & Tillage Research*, 2017; 171: 1–8.
- [3] Jin C, Nan Z R, Wang H C, Jin P. Plant growth and heavy metal bioavailability changes in a loess subsoil amended with municipal sludge compost. *Journal of Soils & Sediments*, 2017; 17: 2797–2809.
- [4] Wang Z Q, Hu Y X, Wang R, Guo S L, Du L L, Zhao M, et al. Soil organic carbon on the fragmented Chinese loess plateau: combining effects of vegetation types and topographic positions. *Soil & Tillage Research*, 2017; 174: 1–5.
- [5] Reeves D W, Edwards J H, Elkins C B, Touchton J T. In-row tillage methods for subsoil amendment and starter fertilizer application to conservation-tilled grain sorghum. *Soil & Tillage Research*, 1990; 16: 359–369.
- [6] Zhao J L, Wang X G, Lu Y, Wei Y P, Guo M Z, Fu J. Biomimetic earthworm dynamic soil looser for improving soybean emergence rate in cold and arid regions. *Int J Agric & Biol Eng*, 2021; 14(3): 22–31.
- [7] Ren L Q, Han Z W, Li J Q, Tong J. Experimental investigation of bionic rough curved soil cutting blade surface to reduce soil adhesion and friction. *Soil & Tillage Research*, 2006; 85: 1–12.
- [8] Zhao J L, Guo M Z, Lu Y, Huang D Y, Zhuang J. Design of bionic locust mouthparts stubble cutting device. *Int J Agric & Biol Eng*, 2020; 13(1): 20–28.
- [9] Yan G Q, Tian P, Mo J S, Xie H, Wei H L. Low-velocity resistance distortion and bionic drag reduction for ship-type paddy field machinery. *Int J Agric & Biol Eng*, 2020; 13(2): 7–14.
- [10] Huang W H, Li M, Ge C, Wei L J, Niu Z J, Zhu X Z. Optimization design and experimental analysis of bionic viscosity reduction of chisel type energy saving subsoiling shovel. *Journal of Physics: Conference Series*, 2020; 1635(1): 12036–12041.
- [11] Zhang J B, Tong J, Ma Y H. Design and experiment of bionic anti-drag subsoiler. *Transactions of the CSAM*, 2014; 45(4): 141–145. (in Chinese)
- [12] Zhang J B, Tong J, Ma Y H. Abrasive wear characteristics of subsoiler tines with bionic rib structure surface. *Journal of Jilin University (Engineering and Technology Edition)*, 2015; 45(1): 176–180. (in Chinese)
- [13] Jia H L, Guo M Z, Zhao J L, Huang D Y, Zhuang J, Qi J T. Design and test of bionic wide-ridge soybean tilling-sowing machine. *Int J Agric & Biol Eng*, 2019; 12(1): 42–51.
- [14] Zhao J L, Lu Y, Guo M Z, Fu J, Wang Y J. Design and experiment of bionic stubble breaking-deep loosening combined tillage machine. *Int J Agric & Biol Eng*, 2021; 14(4): 123–134.
- [15] Tong J, Moayad B Z, Ma Y H, Sun J Y, Chen D H, Jia H L, et al. Effects of biomimetic surface designs on furrow opener performance. *Journal of Bionic Engineering*, 2009; 6(3): 280–289.
- [16] Wu L Y, Jiao Z B, Song Y Q, Liu C H, Wang H, Yan Y Y. Experimental investigations on drag-reduction characteristics of bionic surface with water-trapping microstructures of fish scales. *Scientific Reports*, 2018; 8: 12186–12191.
- [17] Ma F L, Zeng Z Z, Gao Y M, Liu E Y, Xue Q J. Research status and progress of bionic surface drag reduction. *China Surface Engineering*, 2016; 29: 7–15. (in Chinese)
- [18] Pu X, Li G, Liu Y. Progress and perspective of studies on biomimetic shark skin drag reduction. *Chem Bio Eng Reviews*, 2016; 3: 26–40.
- [19] Sun J Y, Wang Y M, Ma Y H, Tong J, Zhang Z J. DEM simulation of bionic subsoilers (tillage depth >40 cm) with drag reduction and lower soil disturbance characteristics. *Advances in Engineering Software*, 2018; 119: 30–37.
- [20] Muthuchamy M, Govindan R, Muneeswaran M, Song J M, Natesan M. Biologically synthesized zinc oxide nanoparticles as nanoantibiotics

- against ESBLs producing gram negative bacteria. *Microbial Pathogenesis*, 2018; 121: 224–231.
- [21] Wainwright S A, Vosburgh F, Hebrank J H. Shark skin: Function in locomotion. *Science*, 1987; 202(4369): 747–749.
- [22] Hang C G, Huang Y X, Zhu R X. Analysis of the movement behaviour of soil between subsoilers based on the discrete element method. *Journal of Terramechanics*, 2017; 74: 35–43.
- [23] Hang C G, Gao X J, Yuan M C, Huang Y X, Zhu R X. Discrete element simulations and experiments of soil disturbance as affected by the tine spacing of subsoiler. *Biosystems Engineering*, 2017; 168: 73–82.
- [24] Günther W, Horst E. The application of Mohr-Coulomb soil mechanics to the design of winged shares. *Journal of Agricultural Engineering Research*, 1997; 67(3): 235–247.
- [25] Han Y, Aboulsleiman Y N, Hull K L, Al-Muntasheri G A. Numerical modeling of elastic spherical contact for Mohr-Coulomb type failures in micro-geomaterials. *Experimental Mechanics*, 2017; 57(2): 1–15.
- [26] Leary P, Zsombor P. Direct and specific least-square fitting of hyperbol and ellipses. *Journal of Electronic Imaging*, 2004; 13(3): 492–503.